Design of β-Hairpin Peptides for Modulation of Cell Adhesion by β-Turn Constraint

Sumana Giddu,[†] Vivekanandan Subramanian,[§,‡] Ho Sup Yoon,[§] and Seetharama D. Satyanarayanajois*[,†]

Department of Basic Pharmaceutical Sciences, University of Louisiana at Monroe, 700 University Avenue, Monroe, Louisiana 71209, and Division of Structural and Computational Biology, School of Biological Sciences, Nanyang Technological University, Singapore 637551

Received July 7, 2008

The CD2−CD58 interaction in immune regulation and disease pathology has provided new targets for developing potential immunosuppressive agents. In the present study, we report the introduction of constraints to generate β-hairpin structures from the strand sequences of CD2 protein. The β-hairpin structures were induced in the designed peptides by introducing Pro-Gly sequences in the peptides. Results from NMR and MD simulation indicated that the peptides exhibited β-turn structure at the X-Pro-Gly-Y sequence and formed the β-hairpin structure in solution. The ability of these peptides to inhibit cell adhesion was evaluated by two cell adhesion assays. Among the peptides studied (**1**−**4**) (P1−P4), peptides **2**−**4** were able to inhibit cell adhesion between Jurkat cells and SRBC nearly 50% at 180 μM, and 80% inhibition between Jurkat cells and Caco-2 cells was seen at 90 μM. Peptide **1** did not show significant inhibition activity compared to control.

Introduction

Protein−protein interactions play a major role in several cellular processes, including adhesion between cells for immune response, tight junctions that hold the blood−brain barrier, and attachment of different proteins to endothelial cells. The interaction between T cells and APC[a] is a complex process involving several adhesion molecules.[1] Adhesion molecules, or costimulatory molecules, help to sustain contact between T cells and APC; help T-cell receptor−major histocompatibility complex (TCR−MHC) interactions to generate signals for immune response.[2−4] Among the different cell adhesion molecules that participate in immunological response, CD2 and its ligand CD58 (LFA-3) are two of the best-characterized. CD2 plays an important role in mediating antigen-dependent or antigen-independent T-cell activation with dual functions of adhesion and signal transduction.[5,6] During the earliest stage of T cell and APC contact, the ligation of CD2 by CD58 creates an intercellular membrane distance (∼135 Å) ideal for TCR−MHC complex, allowing TCR to diffuse into the contact space and interact with peptide−MHC (pMHC).[7] In the presence of CD2−CD58 interaction, T cells recognize correct pMHC with a 50- to 100-fold greater affinity than in the absence of this interaction.[8] Thus, a better understanding of the critical roles of CD2−CD58 interaction in immune regulation and disease pathology provides an opportunity to design new potential immunosuppressive agents.

In vitro studies have suggested that anti-CD2 blocking antibodies inhibit T-cell activation when added to mixed lymphocyte reaction. Inhibition of the CD2−CD58 interaction has important implications in controlling immune responses in autoimmune diseases.[9−11] Therefore, molecules designed to inhibit CD2−CD58 interaction may function as immunosuppressants. There are several reports of modulation of CD2−CD58 interactions for therapeutic use. The hybridoma cells producing mouse antirat CD2 mAb (OX34, IgG2a) treatment can prevent the induction of arthritis[12] and prolong graft survival, acting synergistically with cyclosporine.[13] Alefacept (Biogen Inc., Cambridge, MA), a soluble CD58-Ig fusion protein designed to disrupt the T-cell activation process via interrupting CD2−CD58 interaction, has been approved by the U.S. Food and Drug Administration to treat plaque psoriasis. Alefacept showed clinical efficacy in reducing the signs and symptoms of joint inflammation in patients with psoriatic arthritis.[14,15] The rat CD2 mAb, BTI-322, and its humanized version, MEDI-507, effectively inhibited the primary xenogeneic mixed lymphocyte reaction in vitro, suggesting the potential of the CD2 mAb for tolerance induction and T-cell depletion in vivo.[16] BTI-322 was found to be effective in renal allograft tolerance and acute graft versus host disease in clinical studies,[17,18] while MEDI-507 is now being studied for the treatment of certain lymphoproliferative disorders and psoriasis.[19] These findings make CD2 and CD58 molecules attractive targets for understanding the mechanism of cell adhesion inhibition and autoimmune diseases.[20−22]

In our previous work, we have shown that peptides designed from the β-turn and β-strand region of CD2 (Figure 1a) could modulate CD2−CD58 interactions.[23−26] The peptides designed from the β-strand region were from discontinuous regions of CD2 protein. The two strands were linked by a peptide bond or disulfide bond (Figure 1b). In the present study, we report the introduction of constraints (Pro-Gly sequence and cyclization) to generate β-turn structures from the strand sequences [27−29] (Figure 1b, Table 1). Our NMR and molecular modeling results indicated that peptides **1**−**4** exhibited β-turn structure at X-Pro-

* To whom correspondence should be addressed. Phone: (318) 342-1993. Fax: (318) 342-1737. E-mail: jois@ulm.edu.
[†] University of Louisiana at Monroe.
[§] Nanyang Technological University.
[‡] Present address: Structural Biology/NMR Spectroscopy, NIH/FDA, Bethesda, Maryland 20892.

[a] Abbreviations: AET, 2-aminoethylisothiouronium hydrobromide; APC, antigen-presenting cells; BCECF-AM, bis-carboxyethylcarboxyfluorescein acetoxymethyl; BSA, bovine serum albumin; CD, cluster of differentiation; DIPEA, *N*,*N*′-diisopropylethylamine; DMSO, dimethyl sulfoxide; FBS, fetal bovine serum; FITC, fluorescein isothiocynate; fs, femtosecond; HATU, 2-(7-aza-1*H*-benzotriazole-1-yl)-1,1,3,3-tetramethyluronium hexafluorophosphate; hCD2, human CD2; hCD58, human CD58; MD, molecular dynamics; MEM-α, minimum essential medium-α; MHC, major histocompatibility complex; pMHC, peptide−MHC; MTT, [3-(4,5-dimethylthiazol-2-yl)-2,5-diphenyl tetrazolium bromide]; MTT assay, mitochondrial dehydrogenase activity assay; PAL-resin, 5-(4-aminomethyl-3,5-dimethoxyphenoxy)valeryl-resin; Pen, β,β-dimethylcysteine; ps, picosecond; rmsd, root-mean-square deviation; SRBC, sheep red blood cells; TFA, trifluoroacetic acid. Three-letter abbreviations were used for amino acids in the peptides in the text, and a single letter abbreviation was used for amino acids in protein CD2 and in figures and tables for convenience.

10.1021/jm8008212 CCC: $40.75
Published on Web 01/05/2009

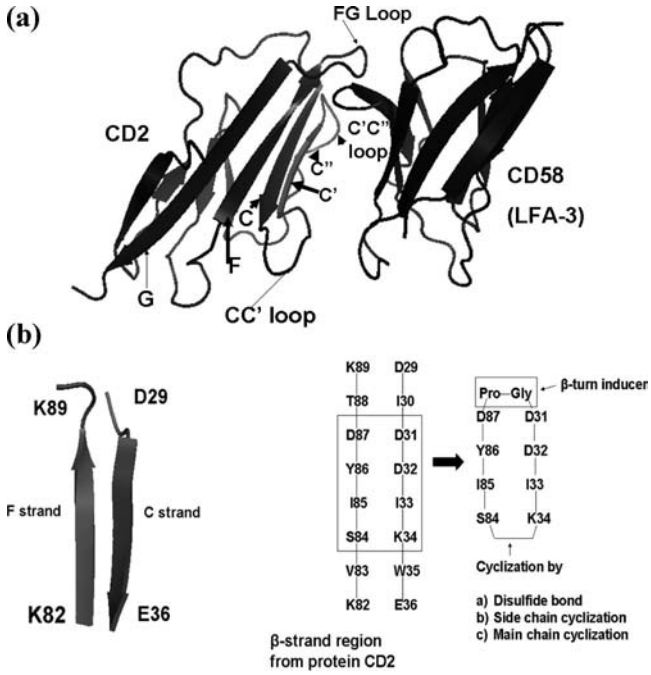

Figure 1. (a) Ribbon diagram of crystal structure of hCD2−hCD58 (LFA-3) complex showing different strands of β-sheet. The proposed energetic hot-spot and its surroundings in the hCD2−hCD58 interface are shown. (b) Design of peptides: F and C β-strands from CD2 crystal structure; peptides from the discontinuous epitopes of the CD2 protein. The residues in this region are important in binding to CD58. Note that in the cyclic peptides the two strands are joined by a peptide bond or disulfide bond.

Gly-Y sequence and formed the β-hairpin structure in solution. These peptides were also able to inhibit cell adhesion interaction between Jurkat cells and SRBC and between Jurkat and Caco-2 cells.

Results

Peptides from CD2 β-Strand Region Were Able To Inhibit Cell Adhesion between T Cells and Epithelial Cells. Jurkat cells express CD2, and Caco-2 cells express CD58 protein. The ability of peptides **1**−**4** to inhibit cell adhesion was evaluated by lymphocyte-epithelial assay[30] as shown in Figure 2. Peptides **2**−**4** showed nearly 80% inhibition at 90 μM, whereas peptide **1** showed only 30% inhibition at 90 μM. A control peptide showed less than 20% inhibition. Peptides **2**−**4** showed concentration dependence of cell adhesion inhibition. CD58 antibody was used as a positive control. Anti-CD58 showed 100% inhibition at a concentration of less than 5 μM. Statistical analysis of the data indicated that there was a significant difference in the inhibition activity of peptides **2**−**4** compared to that of control ($P < 0.05$). However, there was no statistical difference in the activity between peptide **1** and control. When we compared the activities of peptides **2**−**4** at 90 μM, there was no statistical difference.

Peptides from CD2 β-Strand Region Were Able To Inhibit the E-Rosette Formation between SRBC and T Cells. Sheep red blood cells (SRBC) express CD58, and Jurkat cells express CD2 protein. When these cells are incubated, they adhere to each other. Each Jurkat cell adheres to many sheep red blood cells. Five or more SRBC adhering to a Jurkat cell are counted as positive E-rosetting.[31] The ability of peptides **1**−**4** to inhibit the SRBC and Jurkat cell E-rosette formation is shown in Figure 3. Peptides **2** and **3** were able to inhibit E-rosette formation by nearly 60% at 180 μM compared to the control peptide. Peptide **4** showed 50% inhibition activity at 180 μM, and peptide **1** indicated only 20% inhibition at 180 μM.

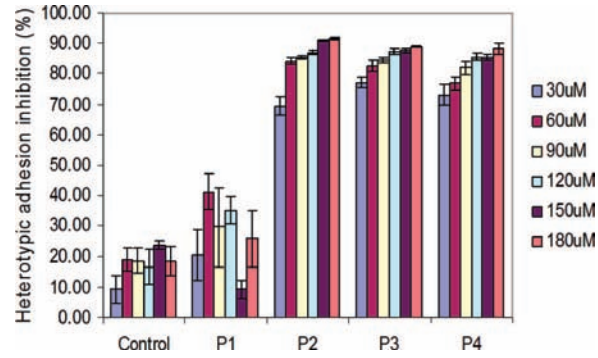

Figure 2. Inhibition of lymphocyte-epithelial adhesion by synthetic peptides derived from CD2 protein. Peptides were added to the confluent Caco-2 monolayer, and then the BCECF-labeled Jurkat cells were added to the mixture. After incubation for 45 min at 37 °C, nonadherent Jurkat cells were removed by washing with PBS, and the monolayer-associated Jurkat cells were lysed with Triton X-100 solution. Soluble lysates were transferred to 96-well plates for reading in a microplate fluorescence analyzer. Values shown are the percent inhibition of peptide-treated cells and are expressed as the mean of three independent experiments. Peptides **1**−**4** are represented as P1−P4.

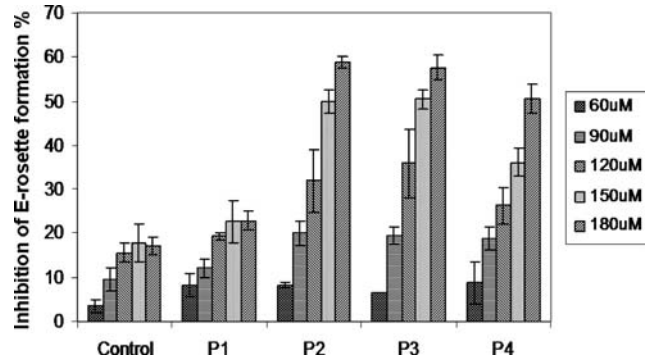

Figure 3. Inhibition of E-rosette formation by synthetic peptides derived from CD2 protein. Peptides were added to AET-treated sheep red blood cells (SRBC) (expressing CD58 protein) first, and then an equal amount of Jurkat cells (expressing CD2 protein) was added later. Cells with five or more SRBC bound were counted as rosettes. Values are percent inhibition of peptide-treated cells and are expressed as the mean of three independent experiments. Peptides **1**−**4** are represented as P1−P4.

Antibody Binding Inhibition Assay. We hypothesized that peptides derived from CD2 protein would inhibit cell adhesion interaction between Jurkat cells and Caco-2/SRBC, presumably by binding to CD58 protein. The ability of these peptides to inhibit anti-CD58 binding to CD58 protein on Caco-2 cells will give us an indication of whether the peptides bind to the same region on CD58 as the antibody does to inhibit CD2−CD58 interaction. To evaluate the ability of CD2 peptides to bind with CD58, we carried out an antibody binding inhibition assay on peptide **2**. Fluorescently labeled anti-CD58 was used to monitor the binding of antibody to Caco-2 cells. Figure 4 shows the ability of peptides to inhibit fluorescently labeled anti-CD58 binding to Caco-2 cells bearing CD58. Peptide **2** was able to inhibit anti-CD58 binding by 45%. We have compared the ability of antibody binding inhibition of peptide **2** with that of a previously reported peptide cAQ (cyclo(1,12)PenAQFRK-EKETFC-OH) from our laboratory.[24]

Cell Viability Assay. The MTT assay, an index of cell viability and cell growth, is based on the ability of viable cells

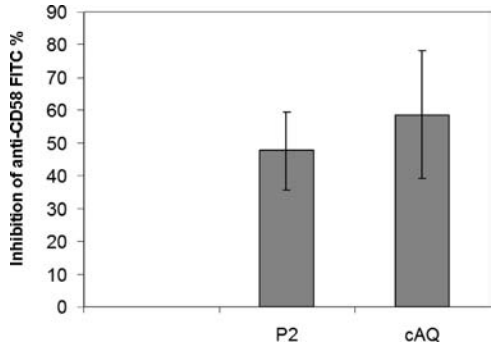

Figure 4. Inhibition of anti-CD58-FITC binding to CD58-bearing Caco-2 cells by synthetic peptides derived from CD2. Inhibition of antibody by peptide **2** and another peptide cAQ is shown in the figure. Caco-2 cells without the peptide and a control peptide were used. Values plotted are the mean values of three independent experiments. Peptide **2** is represented as P2.

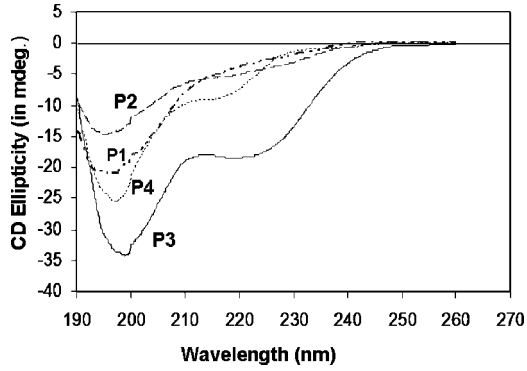

Figure 5. CD spectra of peptides (**1**−**4**) in water at pH 7 at a concentration of 250 μM. The legend for different peptides is shown in the figure. Peptides **1**−**4** are represented as P1−P4.

to reduce MTT from a yellow water-soluble dye to a dark-blue insoluble formazan product by mitochondrial enzymes associated with metabolic activity.[32] The MTT assay is used to evaluate the effect of toxicity of peptides on the cells used in the adhesion assay. In this assay, the ability of the peptides to inhibit the growth of human Caco-2 cells was measured. The results showed that the Caco-2 monolayers incubated with the highest dose of peptides (180 μM) for fixed periods (2 h) in the lymphocyte-epithelial adhesion assay retained more than 80% cell viability (Supporting Information). Therefore, the peptides used in this study were not toxic to the cells, indicating that the mechanisms of the two cell-based adhesion assays may be due to the blocking of CD2−CD58 interaction by these peptides.

Circular Dichroism Studies. Circular dichroism spectra of peptides **1** (Figure 5) showed a negative band around 195 nm, indicating a peptide with less secondary structure. The CD spectrum of peptide **2** showed a negative band around 195 nm and a negative shoulder around 220 nm, indicating a small percentage of sheet type of structure in the peptide. The CD spectra of peptides **2**−**4** showed two negative bands, one around 200 nm and the other around 220 nm. In the case of peptides **3** and **4**, the negative band around 220 nm was intense and is attributed to β-sheet or β-turn-like structure in the peptides.[33−36] Overall, CD studies indicate that peptides **2**−**4** have well-defined secondary structures compared to peptide **1**.

NMR and Structural Studies. To understand the structure−activity relationships of peptides **1**−**4**, NMR studies were carried out in 90% H_2O/10% D_2O. The amide region of the 1D NMR spectrum of the peptide showed good dispersion of chemical shifts for peptides **1**−**4**. NMR proton chemical shifts of peptides **1**−**4** are available as Supporting Information. Linear peptides and cyclic peptides with a cyclic ring size of hexapeptide or larger show flexible conformation in solution. The observed NMR spectral parameters (chemical shift, coupling constant, and ROE) are averaged values of the conformers that exist in solution. These peptides may or may not show "ideal" ROE cross-peaks for a β-strand structure. Hence, on the basis of the NMR data and NMR restrained molecular dynamics simulations, the most probable structures of the peptides in solution are proposed.

Peptide 1. The NMR spectrum of peptide **1** was well resolved, and all the amino acids in the peptide could be identified with corresponding peaks in TOCSY[37] and ROESY.[38] The ROESY spectrum of peptide **1** showed sequential connectivities between $C_\alpha H(i)-NH(i+1)$ residues. The amide−amide region of the ROESY spectrum (Supporting Information) showed connectivities from the NH of Ser2 to the NH of Ile3, the NH of Tyr4 to the NH of Asp5, and the NH of Ile10 to the NH of Lys11, indicating a possible folded structure of the peptide. There was one long-range ROE between the NH of Asp5 and the NH of Lys11, suggesting the possibility of β-strand-type structure. The aliphatic region of the ROESY spectra of peptide **1** showed a ROE cross-peak between the $C_\alpha H$ of Asp5 and $C_\delta H$ of Pro6, suggesting that the X-pro bond is in trans configuration.[39] The NMR $C_\alpha H$ conformational shifts ($\Delta\delta_{C\alpha H}$)[40] and chemical shift index[41] indicated structured peptides in solution. In peptide **1**, residues from Ser2-Asp5 showed a positive chemical shift index indicative of β-strand structure. However, the remaining part of the peptide showed a negative chemical shift index, suggesting the β-turn structure of the peptide. Most of the residues showed positive values of chemical shift from random coil chemical shift values indicative of β-strand structure of the peptide (Figure 6a). The coupling constants were in the range of 6−8 Hz, suggesting rapidly interconverting conformations of the peptide that exists in solution.[42] The temperature coefficients of the chemical shift of amide resonances of Ile3 and Gly7 were <4 ppb/K, suggesting that these may be intramolecularly hydrogen-bonded or solvent-shielded amide protons (Figure 6a).[43]

The possible conformation of peptide **1** was generated using ROESY NMR data. To carry out the molecular dynamics simulation for peptide **1**, a total of 55 distance constraints from NMR data of peptide were used. Eleven low energy structures that were consistent with NMR data were selected as representative structures (Figure 7A). Structural statistics are shown in Table 2. The structure exhibited a type II β-turn at Asp5-Pro6-Gly7-Asp8.[44] The β-turn was stabilized by an intramolecular hydrogen between the NH of Asp8 and carbonyl group of Asp5. The peptide has strand like structure from Ser2 to Asp5 and Asp8 to Cys12. The two strands were stabilized by hydrogen bonds between the NH of Ile3 to C═O of Ile10 and the NH of Cys12 to C═O of Cys1. The concept of a hydrogen bond at Ile3 NH was supported by the low temperature coefficient of chemical shift of NH of Ile3. A kink in the strand was observed at Ile3 with a γ-turn around Ile3 and hydrogen bonding from the NH of Tyr4 to the C═O of Ser3.

Peptide 2. The $C_\alpha H$ chemical shifts of peptide **2** from random coil values were negative for all the residues in the peptide except S2 and D5 (Figure 6b). The chemical shift index of residues from Pro6 to Asp9 was negative, supporting the presence of β-turn structure of the peptide in solution. The amide−amide region of the ROESY spectrum showed several

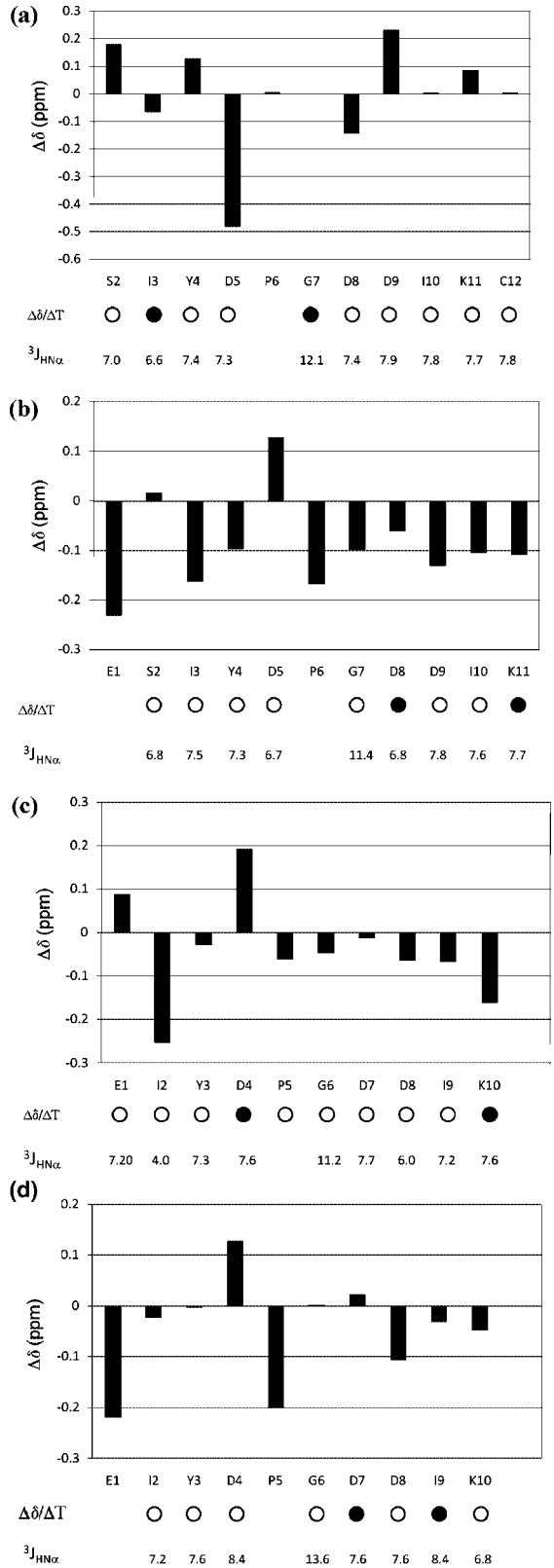

Figure 6. A plot of the deviations of $C^{\alpha}H$ chemical shift values of peptides **1**−**4** (a−d) from random coil values ($\Delta\delta$ = (observed $\delta_{\alpha H}$) − (random-coil $\delta_{\alpha H}$)). Chemical shift values of random coil were obtained from ref 42. Observed coupling constant values ($^3J_{HN\alpha}$ in Hz) and temperature coefficients of chemical shift for amide protons ($\Delta\delta/\Delta T$ in ppb/K) are also shown. ($\Delta\delta/\Delta T$) > 4 ppb/K are represented as open circles, indicating solvent-exposed protons. ($\Delta\delta/\Delta T$) < 4 ppb/K are represented as closed circles, indicating solvent-shielded or participation in intramolecular hydrogen bonding.

sequential ROE connectivities. The ROE connectivity between the NH of Gly7 and NH of Asp8 also supported the β-turn structure. The coupling constants $^3J_{HN\alpha}$ were in the range of 6−8 Hz as observed in most peptides that undergo rapid interconversion of conformations in solution.[42]

A total of 80 intra- and inter-residue ROEs were used in the calculation of the structure of peptide **2**. The conformation of the peptide derived from NMR and molecular modeling exhibited two consecutive β-turns, one at Asp5-Pro6-Gly7-Asp8 and another at Pro6-Gly7-Asp8-Asp9. The dihedral angles at these residues indicated that it is a type II β-turn. The peptide exhibits a strand type of conformation from Glu1 to Asp5 and from Asp9 to Lys11, giving a β-hairpin structure.[45,46] The peptide was stabilized by three hydrogen bonds in the strands and β-turn region: Asp9 NH with Asp5 C═O, Asp5 NH with Asp9 C═O, and Lys11 NH with Asp9 C═O. An additional hydrogen bond was observed between the NH of Asp8 and the Pro6 C═O. Structural statistics and Ramachandran plot analysis of the structure are shown in Table 2. The average backbone rmsd of 16 structures was 0.066 Å for peptide **2**, indicating the stability of the low energy structure for the peptide in solution. The 16 structures of peptide **2** superimposed on its average structure are shown in Figure 7B.

Peptide 3. Peptide **3** was cyclized by a main-chain peptide bond between Glu1 and Lys10. The 2D TOCSY NMR spectrum of this cyclic peptide showed the resonances for all the amides in the amino acid sequence, including Glu1. The ROESY spectrum of the peptide showed sequential connectivities between the NH of Glu1 and $C_{\alpha}H$ of Lys10, indicating main-chain cyclization with no free amino or carboxyl ends. The $C_{\alpha}H$ chemical shifts of peptide **3** from random coil values were negative for most of the residues in the peptide except Asp4 and Glu1, which suggests a stable β-turn structure of the peptide in solution (Figure 6c). The $^3J_{HN\alpha}$ coupling constant values of residues Glu1, Asp4, Asp7, Ile9, and Lys10 were >7.5 Hz, indicating a strand type of structure in the peptide. The Ile2 showed a coupling constant of 4 Hz, which suggested a folded structure around Ile2. The temperature coefficient of chemical shift of Lys10 and Asp4 was <4 ppb/K, suggesting solvent-shielded amide protons for these residues. The NH−NH region of the ROESY spectrum exhibited cross-peaks between the NH of Ile2 and the NH of Tyr3, NH of Tyr3 and NH of Asp4, NH of Glu1 and NH of Lys10, NH of Asp7, and NH of Asp8, as well as NH of Gly6 and NH of Asp7. The ROE between the NH of Gly6 and NH of Asp7 supports a β-turn structure of the peptide around Asp4-Pro5-Gly6-Asp7.

Eighty-five intra- and inter-residue ROEs were employed in the calculation of the structure of peptide **3** using NMR constrained molecular dynamics and energy minimization. A total of 16 structures were superimposed on their average structure and are shown in Figure 7C. The peptide exhibits a β-turn at Asp4-Pro5-Gly6-Asp7; however, this β-turn was type I with dihedral angles around Pro5, $\Phi = -65$, $\Psi = -44$, and Gly6, $\Phi = -74$, $\Psi = 0$. The β-turn was stabilized by hydrogen bonding between the NH of Asp7 and C═O of Asp4. A β-turn was also observed at Glu1-Ile2-Tyr3-Asp4, but it was not stabilized by intramolecular hydrogen bonding. The overall structure of peptide **3** was a twisted β-strand with a β-turn. The β-strands were stabilized by hydrogen bonds between the NH of Ile9 and Asp7 side chain C═O.

Peptide 4. Peptide **4** has sequence similar to that of peptide **3**. However, the cyclization was achieved by side chains of Glu1 and Lys10. The TOCSY NMR spectrum of peptide **4** was different from that of peptide **3**. The amide resonances of Ile2,

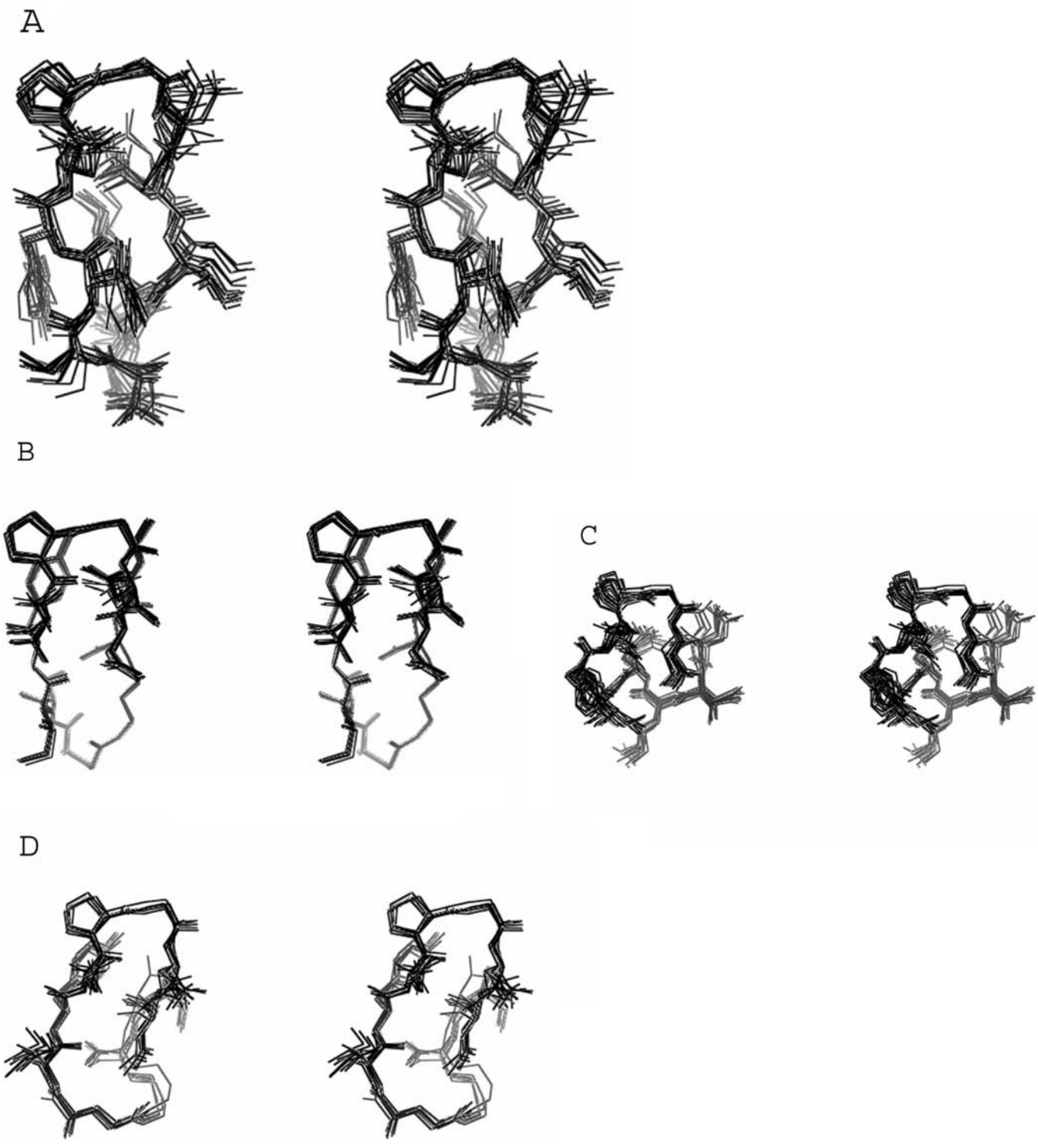

Figure 7. Stereoview of overlapped energy minimized structures of peptides (**1**−**4**) (A−D). See text for details about the number of structures.

Table 1. Sequences of the Peptides That Are Derived from Human CD2 Protein

code	sequence	comment
1	cyclo(1,12)Pen^{1}S^{2}I^{3}Y^{4}D^{5}P^{6}G^{7}D^{8}D^{9}I^{10}K^{11}C^{12}-OH	disulfide bond cyclization
2	cyclo(1,11)H-E^{1}S^{2}I^{3}Y^{4}D^{5}P^{6}G^{7}D^{8}D^{9}I^{10}K^{11}-OH	cyclized by side chain of E1 and K11
3	cyclo(1,10)E^{1}I^{2}Y^{3}D^{4}P^{5}G^{6}D^{7}D^{8}I^{9}K^{10}	main chain cyclization
4	cyclo(1,10)H-E^{1}I^{2}Y^{3}D^{4}P^{5}G^{6}D^{7}D^{8}I^{9}K^{10}-OH	cyclized by side chain of E1 and K10
control	KGKTDAISVKAI-NH_2	reversal of sequence and replacement of Y81 and Y86 by Ala

Tyr3, and Asp4 were shifted downfield compared to the chemical shifts of peptide **3**, indicating the effect of cyclization on the conformational parameters observed by NMR. The Gly6 $C_\alpha H$ protons were well separated, suggesting the stable structure around Gly6. The $C_\alpha H$ chemical shifts of Asp4, Gly6, and Asp7 were positive from random coil values; for the remaining residues in peptide **4**, they were negative (Figure 6d). This clearly indicates that the peptide acquires β-strand and β-turn

Table 2. Structural Statistics for Peptides **1**−**4**

parameter	peptide **1**	peptide **2**	peptide **3**	peptide **4**
total number of ROEs and cyclization constraints used for calculations	55	80	85	80
number of intraresidue ROEs	37	55	64	61
number of inter-residue ROEs	18	25	21	19
number of NOE violations greater than 0.5 Å	0	0	0	0
	Ramachandran Plot			
number of residues in favored region	79%	71%	72%	84%
number of residues in allowed region	100%	100%	100%	100%
number of outliers	0%	0%	0%	0%
rmsd of backbone atoms (Å)	0.455	0.066	0.304	0.404
rmsd of all atoms	0.736	0.401	0.606	1.072

conformations in solution. The chemical shift indices of Pro5 and Asp8 were negative, and the remaining residues showed either zero or positive chemical shift index values, pointing to the possibility of a β-turn around Pro-Gly and β-strand in the remaining part of the peptide sequence. The coupling constant, $^3J_{HN\alpha}$, for most of the amino acid residues in the peptide was >7.5 Hz, with Ile9 exhibiting a coupling constant of 8.4 Hz due to β-strand type of structure. The temperature coefficients of the chemical shifts of Asp7 and Ile9 were <4 ppb/K, suggesting solvent-shielded amides of these residues (Figure 6d). The NH−NH region of the ROESY spectrum indicated sequential connectivities from the NH of Gly6 to the NH of Lys10.

A total of 80 intra- and inter-residue ROEs were used in the structure calculation of peptide **4**. An ensemble of 15 low-energy structures that satisfy the NMR data superimposed with their average structure is shown in Figure 7D. The rmsd of the backbone atoms of 15 structures compared to the average structure was 0.404 Å. The overall structure of peptide **4** was similar to the structures of peptides **2** and **3**. The dihedral angles at Pro5 and Gly6 indicated that the peptide **4** acquired a type II β-turn structure. The β-turn was stabilized by an intramolecular hydrogen bond between the NH of Asp7 and the C═O of Asp4 and also between the NH of Asp8 and the C═O of Asp4. The possibility of an intramolecular hydrogen bond at Asp7 was supported by the low temperature coefficient of chemical shift of Asp7 NH. Residues Ile2, Tyr3, Asp4, Asp7, and Asp8 exhibited extended conformation, giving the peptide a strand type of structure from Glu1 to Asp4 and from Asp7 to Asp8.

Discussion

Design of Peptides. The crystal structure of the CD2−CD58 complex indicated that the interaction surface of CD2 with CD58 has two β-strand structures (F and C) with charged residues in CD2 protein.[6,8,47] The β-strands span eight to nine amino acid residues. These strands (F and C) are discontinuous in sequence (residues 29−36 and 82−89) but spatially close and form an antiparallel β-sheet (Figure 1) in which strands are 5 Å apart. By use of mutagenesis studies, the residues in these strands have been shown to be important in binding CD2 to CD58 protein.[47] Point mutation studies suggested that in hCD2 the Y86 to A86 mutation (F strand) resulted in a significant loss of binding of CD2 to CD58 (more than 1000-fold), while Y86 to F86 mutation in the same region did not affect the binding. The ε-amino group of K34 in CD58 (Figure 1b) is involved in hydrogen-bond formation to D32 of CD2, which helps K34 maintain an extended conformation, thereby ensuring the formation of a small hydrophobic core. This region is identified as the energetic hot-spot of the CD2−CD58 interaction.[47] The aromatic ring of Y86 in CD2 (Figure 1b) and F46 in CD58 create a small but critical hydrophobic core in the CD2−CD58 interface, which is important to the cation−π interaction between the CD2 Y86 aromatic ring and the positively charged ε-amino group of CD58 K34. We proposed that in our peptide design from CD2 protein sequence, if we retain the C strand of CD2 with D31, D32, and K34 residues that are close to the hydrophobic region (CD2 and CD58 both have K34 residue) and the F strand with hot-spot Y86, the peptide will mimic the native structure of the protein.

On the basis of the results mentioned above and our previous studies,[23−26] we proposed that a cyclized β-hairpin peptide assembling the two strands (residues 31−34 and 84−87) (Figure 1b) would be a suitable model for mimicking the CD2 interface with CD58. While designing the peptides, the following important factors were considered: (1) the conformational feature of β-turn/strand and residues that are important in binding to CD58 should be preserved and (2) the backbone flexibility of the peptide should be constrained. It is known that β-hairpin structures are stabilized by β-turns[27,28] or β-turn structures nucleate the hairpin structures in proteins. Pro-Pro and Pro-Gly sequences have been shown to form β-turn structures in proteins and peptides.[48] A Pro-Gly sequence was inserted to connect the two strands between D31 and D87. The other end of the strand (K34-S84) was cyclized by different strategies to acquire a stable peptide structure (Figure 1b, Table 1). Peptide **1** was cyclized via a disulfide bond by introducing penicillamine (Pen) at the N-terminal and Cys at the C-terminal. Peptides cyclized through a disulfide bond located at the strand termini have been reported to form β-hairpin structures.[49,50] In peptides **2**, **3**, and **4**, an amino acid Glu was introduced at the N-terminal. Cross-strand charged residue pairs DK, DR, EK, and ER are statistically favored in antiparallel β-sheets. In β-hairpins, an interaction between positively and negatively charged groups at N and C termini was shown to contribute to β-hairpin stability.[51] In our CD2 peptides, the C-terminal had a Lys residue (Figure 1b). To complement the Lys residue, introduction of Glu at the N- terminal is justified. In the CD2−CD58 interaction, K34 played a major role in forming π−cation interaction with hydrophobic residues. To understand the importance of a Lys side chain in binding, we cyclized the peptide using side chain cyclization as well as main-chain peptide bond cyclization. In peptides **2** and **4**, side chain cyclization was used, and main-chain (end-to-end) cyclization was carried out in peptide **3**. In peptides **1** and **2** Ser was retained. While Ser84 may not play a major role in CD2−CD58 interaction, it is known that the introduction of hydrophilic residues in the peptides increases β-sheet propensity.[51] Thus, with the existing residues in the protein sequence of CD2 β-strand and introduction of β-hairpin-forming and β-turn-inducing sequences, we designed the four peptides shown in Table 1. The control peptide was designed on the basis of the sequence of CD2 in the CD2−CD58 interaction surface, which was defined as the hot-spot. The

sequence was reversed, and the important residues Tyr81 and Tyr86 were replaced with Ala to generate the sequence of the control peptide (Table 1).

Cell Adhesion Inhibition Activity and Structural Studies. Cell adhesion inhibitory activity of peptides **1**−**4** was evaluated using the lymphocyte-epithelial cell adhesion assay and E-rosetting assay.[30,31] The results indicated that peptides **2**−**4** potentially inhibited the cell adhesion activity (nearly 80%) at 90 μM concentration (Figure 2). Statistical analysis indicated that the inhibition activity of peptides **2**−**4** was significant compared to that of the control peptide. There was no difference in the activity of peptides **2**−**4** within that group. Peptide **1** did not show significant inhibition of activity compared to the control peptide. All the peptides described in this work are derived from the β-strand region of CD2 protein.[47] However, as reported above, peptides **1**−**4** are different in the way they are cyclized. NMR and structural studies showed that the peptides exhibit β-turn structure around the Pro-Gly sequence. It is not clear from these studies why peptide **1** does not show cell adhesion inhibition activity although the overall structures of the peptides **1**−**4** are similar. CD studies indicated that peptide **1** exhibits open or unordered structure with a negative band around 195 nm, whereas peptides **2**−**4** exhibit CD spectra with two negative bands, one around 195−200 nm and a second negative shoulder/band around 220 nm, indicative of β-strand or β-turn structure. From the biological activity of the peptides, it is clear that the disulfide bonded constraint may not be suitable for the peptide activity in this particular case. The SAR of peptides **2**−**4** clearly suggests that either main-chain peptide bond cyclization or side-chain cyclization could be used to retain the biological activity in these peptides. To understand the effect of flanking residues to Tyr, an important residue for biological activity, Ser and Ile were retained in peptide **2** (in CD2 protein S84, I85 and Y86) and peptide **4** was designed with the Ser residue removed. The results from cell adhesion inhibitory activity and molecular modeling data indicated that the activity of the peptide was not affected by removal of the Ser residue in the peptide. Peptides **2** and **4** showed similar inhibitory activity. Comparison of the structures of peptides **1**−**4** (Figure 7) with the fragment of protein (C and F strands) CD2 indicated that peptides **1**−**4** acquire a type of structure similar to the crystal structure of CD2 protein. To explain the significantly lower inhibitory activity of peptide **1** compared to peptides **2**−**4**, NMR-derived three-dimensional structures of peptides **1**−**4** were analyzed in terms of overall conformation of the peptides and orientation of Asp, Asp, Lys, and Tyr residues in the peptides. Stability of peptide conformation and enhancement of biological activity of peptides upon cyclization depend on the ring size of the cyclic peptide and method of cyclization (main chain, side chain, or lactam bridge). Peptides cyclized through disulfide bridges at the strand termini have been known to stabilize the β-hairpin structures.[51,52] Peptide **1** with a disulfide bridge cyclization exhibited β-strand structure with a β-turn at Asp5-Pro6-Gly7-Asp8. Compared to peptides **2**−**4**, peptide **1** has a larger ring size with 12 amino acids. Our previous studies indicated that a peptide designed from CD2 β-strand region with 14 amino acids and cyclized by disulfide bond showed 30% inhibitory activity in the cell adhesion inhibition assay.[25] However, the 14-amino acid residue peptide (cyclo(1,14)Pen1-Lys2-Ile3-Asp4-Asp5-Ile6-Asp7-Lys8-Thr9-Asp10-Tyr11-Ile12-Ser13-Cys14) was not stabilized by a Pro-Gly β-turn inducing sequence. Introduction of a Pro-Gly sequence in the peptide and cyclization by disulfide bond did not seem to stabilize the conformation of peptide **1**. Side chain cyclization by Glu-Lys residues and main-chain cyclization by peptide bond seemed to stabilize the overall conformation of the peptides. Thus, the ring size seems to play an important role in the biological activity of the peptides from CD2 described in this study. A recent report on the conformation of β-hairpin structure by disulfide-constrained peptides indicated that the effect of disulfide bonds on β-hairpin stability and biological activity depends on the location of the disulfide bond.[53,54] Thus, placement of disulfide bridge in the design of peptides seems to affect the biological activity of the peptides.

Flexible backbone conformation may influence the orientation of side chains and, hence, the pharmacophore presentation to the receptor. NMR studies indicated that peptide **1** has only 55 distance constraints obtained from ROESY spectra, suggesting the flexibility of conformation of peptide **1** compared to peptides **2**−**4** (Table 2). The flexibility of the backbone conformation of peptide **1** is also supported by the CD spectrum of peptide **1** (Figure 5). Figures 8a−d show the structures of peptides **1**−**4**, highlighting the Tyr, Asp, and Lys residues, which are important for the CD2 protein to interact with CD58. The main difference observed in the conformations of peptides **1**−**4** was the orientation of the Tyr residue with respect to the backbone of the peptides. In peptide **1**, the Tyr side chain χ_1 value was around −60° with the side chain oriented in the downward direction with respect to the β-turn of the peptide (Figure 8a). In peptides **2**, **3**, and **4**, the Tyr side chain was oriented upward toward the β-turn or at a 90° angle to the plane of the β-turn in the peptide. To investigate the dynamic nature of Tyr side chain orientation, a plot of dihedral angle of Tyr χ_1 (Figure 8a inset) vs time was analyzed from the 300 K dynamics data of MD simulations for the peptides. It is very clear that for the entire period of MD simulations of the final structure of the peptide **1**, the dihedral angle χ_1 of the Tyr residue in peptide **1** was around −60°. In peptides **2**, **3**, and **4**, Tyr χ_1 was around −170° or 60°. Different orientation of the Tyr residue in peptide **1** compared to peptides **2**, **3**, and **4** may be responsible for its significantly lower inhibitor activity. (To rule out the possibility of impurities in the peptide **1**, we have carried out LC−MS analysis of peptide **1**. The results indicated that impurities in the peptide were less than 5%). Mutagenesis studies on CD2/CD58 proteins and their adhesion activity have shown that Y86 is very important for cell adhesion activity.[47] The Lys side chain amide did not seem to influence the biological activity in the peptides **1**−**4**. In peptides **2** and **4**, the side chain of Lys was used for cyclization, whereas in peptide **1**, Lys side chain was not used for cyclization. There was no significant difference in the inhibitory activities of peptides **2**, **3**, and **4**. The results from our studies indicate that peptides **2**, **3**, and **4** that we have designed acquire β-hairpin types of structure with Tyr positioned the same in 3D as in the crystal structure protein and that this influences their cell adhesion inhibition activity.

To conclude, we have designed conformationally constrained peptides from CD2 protein using the sequence from the hot-spot region of CD2 protein that is known to bind to CD58. The peptides were shown to inhibit cell adhesion between Jurkat and Caco-2 cells with nearly 80% inhibition at 90 μM. NMR, CD, and molecular modeling studies suggested that these peptides acquire a β-turn structure around the Pro-Gly sequence and that their structures are similar to that of the fragment of CD2 from C and F strands. The biological activity of the peptides was not affected by either side chain or main-chain cyclization. However, disulfide-bonded cyclic peptides seem to lose cell adhesion inhibition activity. Thus, these peptides may

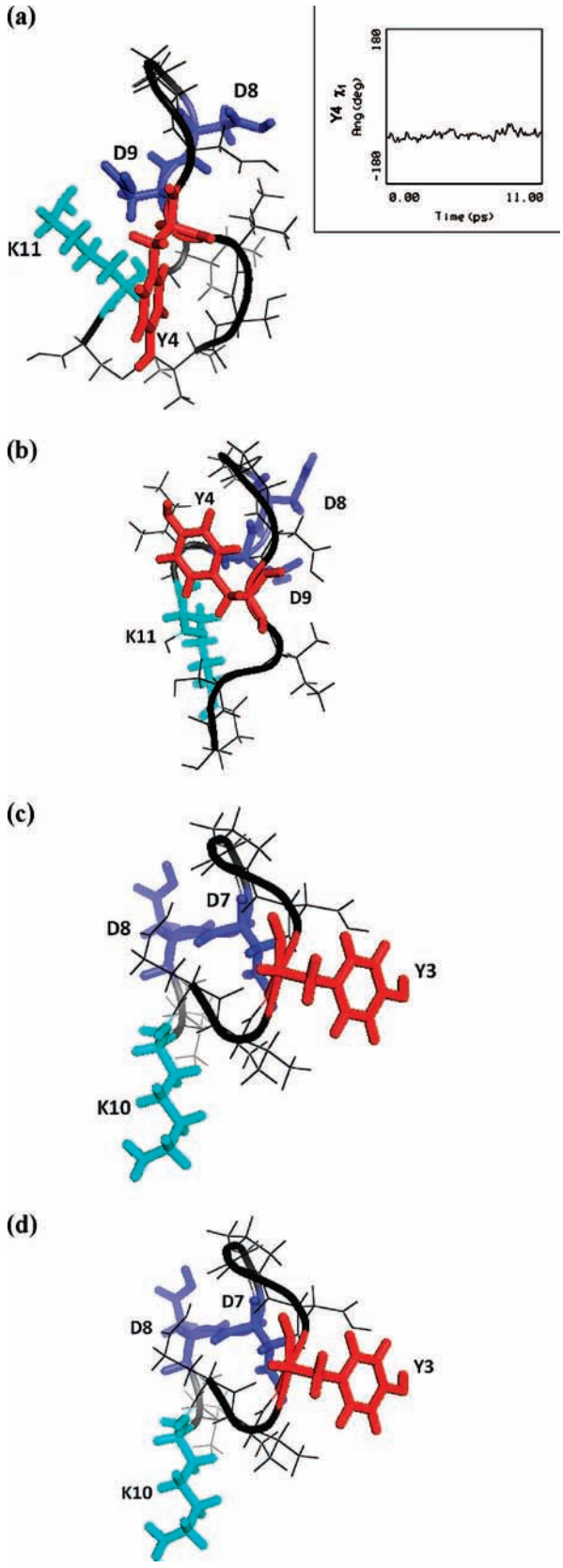

Figure 8. Side view of structures of peptides **1**−**4** (a−d) showing the orientation of Tyr (red), Lys (magenta), Asp and Asp (blue) (in CD2 protein these residues are Y86, K34, D31, D32) with respect to the β-turn of the peptide. The β-turn part of the peptide is facing up in the figure. Notice that in peptide **1**, the Tyr residue is oriented down with respect to the β-turn part of the peptide. Inset in part a shows a plot of χ_1 of tyrosine vs time (11 ps) from NMR-constrained 300 K MD simulation for peptide **1**.

form the lead compounds for designing potential cell adhesion inhibitors to inhibit immune response.

Experimental Section

Peptides. The linear control peptide (Table 1) was designed and synthesized, and the cyclic peptides were purchased from Multiple Peptide Systems (San Diego, CA). The pure products were analyzed by HPLC and electrospray mass spectrometry (ESI-MS). The HPLC chromatogram showed that the purities of peptides were more than 90%, and ESI-MS showed the correct molecular ion for the peptides. Linear control peptides were synthesized using an automatic solid phase peptide synthesizer (Pioneer, Perspective Biosystem) using Fmoc chemistry. The Fmoc-protected amino acids were obtained from Novabiochem (Gibbstown, NJ). All the solvents used in the Pioneer protein synthesizer were obtained from Applied Biosystems (Foster, CA).

Synthesis of Linear Peptide. PAL resin (5-(4-*N*-Fmoc-aminomethyl-3,5-dimethoxyphenoxy)valeryl) was used as a solid support for the linear peptides.[55,56] First, the Fmoc protecting group on the resin was removed by treatment with 20% piperidine/DMF. The N^{α}-Fmoc-amino acids were preactivated by mixing with the coupling reagent HATU/DIPEA (1:1); the activated amino acid was then added to the resin and mixed at room temperature. Cycles of deprotection of Fmoc and coupling with the subsequent amino acids were repeated until the desired peptide-bound resin was completed. The resin was washed manually with DMF, DCM, and methanol successively to remove the excess solvents and dried in vacuo over KOH overnight before cleavage and deprotection. The dried peptidyl-resin was mixed with the cleavage cocktail (90% TFA, 5% thioanisole, and 5% 1,2-ethanedithiol, 5 mL per gram of resin) and precipitated with cold ether. For maximum recovery, the ether−peptide mixture was kept at −20 °C overnight. Then the precipitated material was collected by centrifugation and washed three times with cold ether to remove any residual scavengers. After evaporation of the ether, the peptide was dissolved in water with a few drops of acetic acid and lyophilized.

The lyophilized peptide was dissolved in water/acetonitrile. Peptide was purified by preparative HPLC (waters 600 HPLC system), on a reversed-phase C18 column (Inertsil, 10 mm × 250 mm, 5 μm, 300 Å) with a linear gradient of solvent A (0.1% TFA/H_2O) and solvent B (0.1% TFA/acetonitrile). The peptide was detected by UV at $\lambda = 215$ and 280 nm. The purity of each peptide was verified by an analytical HPLC (Shimadzu LC-10AT VP) using a reversed-phase C18 column (Lichrosorb RP18, 4.6 mm × 200 mm, 10 μm) with the same solvent system as in the preparative HPLC. The molecular weight of the peptides was confirmed by using electrospray ionization mass spectrometry (ESI-MS, Finnigon MAT). The HPLC chromatogram showed that the purity of the peptides was more than 90%, while ESI-MS showed the correct molecular ion for the peptide.

Cell Lines. The Jurkat T-leukemia and the human colon adenocarcinoma cell lines (Caco-2) were obtained from the American Type Culture Collection (Rockville, MD). Jurkat cells were maintained in suspension in RPMI 1640 medium supplemented with 10% heat-inactivated fetal bovine serum (FBS) and 100 mg/L of penicillin/streptomycin. Caco-2 cells were maintained in minimum essential medium-α containing 10% FBS, 1% nonessential amino acids, 1 mM Na pyruvate, 1% L-glutamine, and 100 mg/L of penicillin/streptomycin. Caco-2 cells were used between passages 50 and 60. Sheep blood in Alsever's solution was purchased from Colorado Serum Company (Denver, CO).

Sheep red blood cells (SRBCs) were pelleted by centrifuging about 15 mL of sheep blood in Alsevers solution at 200*g* for 7 min. The pellet was washed three times with phosphate buffered saline (PBS), removing supernatant and buffer coat on each wash. SRBCs were then incubated with four volumes of 2-(2-aminoethyl)isothiourea dihydrobromide (AET) solution at 37 °C for 15 min. The cells were washed three times with PBS and resuspended in RPMI 1640 containing 20% FBS to give a 10% suspension. For use, this cell suspension was diluted 20-fold with RPMI 1640 (20%

FBS). Serial dilutions of peptides in PBS were added to 0.2 mL of 0.5% (w/v) AET treated SRBCs and incubated at 37 °C for 30 min. Then, 0.2 mL of Jurkat cell suspension (2×10^6 cells/mL) was added to the mixture and incubated for another 15 min. The cells were centrifuged (200*g*, 5 min, 4 °C) and incubated at 4 °C for 1 h, after which the cell pellet was gently resuspended and the E-rosettes were counted using a hemacytometer. Cells with five or more SRBCs bound were counted as E-rosettes. At least 200 cells were counted to determine the percentage of E-rosette cells. The inhibitory activity was calculated by using the equation described previously.[30]

Lymphocyte-Epithelial Adhesion Assay. Caco-2 cells were used between passages 50 and 60 and were plated onto 96-well plates at approximately 1×10^4 cells/well. When the cells reached confluency, the monolayers were washed once with MEM-α. Jurkat cells were labeled the same day as the adhesion assay by loading with 2 μM fluorescent dye BCECF at 37 °C for 1 h. Peptide dissolved in MEM-α was added at various concentrations to Caco-2 cell monolayers. After incubation at 37 °C for 30 min, the labeled Jurkat cells (1×10^6 cells/well) were added onto the monolayers. After incubation at 37 °C for 45 min, nonadherent Jurkat cells were removed by washing three times with PBS, and the monolayer-associated Jurkat cells were lysed by incubating with 2% Triton X-100 in 0.2 M NaOH for about 10 min. Soluble lysates were read with a microplate fluorescence analyzer with emission wavelength of 528 ± 20 nm.[57] Data are presented as relative fluorescence or percent inhibition as described previously.[30] Relative fluorescence (FL) was found by reading the values of fluorescence intensity corrected for the reading of background (cell monolayers only).

Statistical analysis of the results from the cell adhesion assay was carried out using Microsoft Excel. Peptides were grouped into **2**−**4** and **1**−**4** and compared with control peptide and within each group. *P* values were compared for analysis.

Antibody Binding Inhibition Assay. About 1×10^4 Caco-2 cells were seeded in 96-well plates and incubated with 180 μM peptides **2** and cAQ for 1 h. Unbound peptide was removed by washing with PBS three times. Two micrograms per milliliter (in PBS) of anti-CD58 FITC (BD Biosciences, Pharmingen, MD) was added to the cells followed by incubation for 1 h. After incubation, unbound anti-CD58 FITC was removed by washing with PBS three times. The monolayer associated was lysed with 2% Triton X-100 in 0.1 M NaOH solution. Soluble lysates were transferred to 96-well plates for reading in a microplate fluorescence analyzer. Plates were read with a 96-well fluorescent plate reader (Biotek, Winooski, VT) with emission wavelength of 528 ± 20 nm. Caco-2 cells without the peptide were used as control. The mean values of the three independent experiments were plotted.

Cell Viability Assay. Peptides that exhibited effects on Jurkat-Caco-2 adherence were tested by MTT assay[32] to determine if their effects were due to its toxicity. A final concentration of 180 μM peptide was added to Jurkat or Caco-2 cells and incubated for $1^1/_2$ h, which is the maximum time of exposure of Caco-2/Jurkat cells during the adherence assay. The cell viabilities were validated by incubating with 15 μL of MTT at 37 °C for 4 h. The MTT-labeled cells were lysed by DMSO, and the absorbance was measured with a microplate reader at a wavelength of 570 nm.

Circular Dichroism Measurement. Circular dichroism experiments were carried out at room temperature on a Jasco J-810 spectropolarimeter flushed with nitrogen. Spectra were collected from 240 to 190 nm using a 1 mm pathlength of cylindrical quartz cell. Each spectrum was the average of three scans taken at a scan rate of 50 nm/min with a spectral bandwidth of 1 nm. The concentration of peptides was varied from 0.15 to 2.5 mM. For the final representation, the baseline was subtracted from the spectrum.

Molecular Dynamics (MD) Simulations. Molecular dynamics simulations and energy minimization were carried out using InsightII/Discover software,[58] version 2000, on a Silicon Graphics computer. Structures of peptides were built using biopolymer module. Consistent valence force field (cvff) was used. NMR restrained molecular dynamics and energy minimization were carried out using simulated annealing procedure.[59] Briefy, NMR upper and lower distances obtained from ROESY data were input as distance constraints to the peptide structure. For cyclization of peptides using backbone or side chain (peptides **2**−**4**), additional constraints were imposed (1.56 Å for upper distance and 1.35 Å for lower distance) for cyclization of peptide bond. The peptide structure was subjected to simulated annealing procedure by increasing the temperature to 900 K, and dynamics was carried out for 10 ps. The history file was analyzed, and five low energy structures were chosen from the history file. Each of these structures was subjected to stepwise dynamics at 800−400 K in steps of 100 K for 5 ps. Finally, each structure was soaked with 10 Å layer of water molecules, and dynamics was carried out at 300 K for 10 ps. A total of 60 structures were generated from this procedure. These 60 structures were compared with each other for similarity using backbone rmsd. These structures were subjected to energy minimization using 100 steps of steepest descent method and 4000 steps of conjugate gradient method (with NMR constraints) until the rms derivative was 0.3 kcal/mol. Twenty structures were chosen from the above 60 structures based on their backbone rmsd, their consistency with ROE data. Structures were further analyzed for intramolecular hydrogen bonding, β-turn structure, and Ramachandran map. The quality of structures was evaluated using the MolProbity[60] online software. The rmsd values of the backbone atoms were compared using MolMol software.[61] Finally, structures with low backbone rmsd were grouped together (11−20 structures) and used for representation of the conformation of the peptides in solution. For calculation of dihedral angles an average structure was chosen from this family of structures. In the case of peptide **1**, constraints for disulfide bond were used for cyclization along with other NMR constraints.[62]

NMR Spectroscopy. The sample for the NMR spectrum of the cyclic peptides was prepared by dissolving 1−2 mg of the peptide in 0.6 mL of 90% H_2O/10% D_2O at the pH with the best dispersion. The one- and two-dimensional NMR experiments were performed and processed on 400 and 600 MHz Bruker DRX spectrometers equipped with a 5 mm probe, at a proton frequency of 400.13 and 600.13 MHz, respectively, using the XWINNMR, version 1.0, software. Spectra were acquired from 290 to 305 K unless otherwise specified. TOCSY,[37] DQF-COSY,[63] and rotating frame nuclear Overhauser spectroscopy (ROESY)[38] experiments were performed by WATERGATE pulse sequence. NMR spectra were analyzed by SPARKY[64] software. Assignment of the spin system was carried out using TOCSY spectrum for each peptide.

Acknowledgment. This research was supported by a startup grant (SJ) from the College of Pharmacy, University of Louisiana at Monroe, LA.

Supporting Information Available: ^{1}H NMR, HPLC, MS, and purity data. This material is available free of charge via the Internet at http://pubs.acs.org.

References

(1) Van der Merwe, P. A.; Davis, S. J. Molecular interactions mediating T cell antigen recognition. *Annu. Rev. Immunol.* **2003**, *21*, 659–684.
(2) Grakoui, A.; Bromley, S. K.; Sumen, C.; Davis, M. M.; Shaw, A. S.; Allen, P. M.; Dustin, M. L. The immunological synapse: a molecular machine controlling T cell activation. *Science* **1999**, *285*, 221–227.
(3) Bromley, S. K.; Burack, W. R.; Johnson, K. G.; Somersalo, K.; Sims, T. N.; Sumen, C.; Davis, M. M.; Shaw, A. S.; Allen, P. M.; Dustin, M. L. The immunological synapse. *Annu. Rev. Immunol.* **2001**, *19*, 375–396.
(4) Bierer, B. E.; Burakoff, S. J. T cell adhesion molecules. *FASEB J.* **1998**, *2*, 2584–2590.
(5) Davis, S. J.; van der Merwe, P. A. The structure and ligand interactions of CD2: implications for T cell function. *Immunol. Today* **1996**, *17*, 177–187.
(6) Davis, S. J.; Ikemizu, S.; Evans, E. J.; Fugger, L.; Bakker, T. L.; van der Merwe, P. A. The nature of molecular recognition by T-cells. *Nat. Immunol.* **2003**, *4*, 217–224.
(7) Zaru, R.; Cameron, T. O.; Stern, L. J.; Muller, S.; Valitutti, S. Cutting edge: TCR engagement and triggering in the absence of large-scale molecular segregation at the T cell-APC contact site. *J. Immunol.* **2002**, *168*, 4287–4291.

(8) Wang, J.; Smolyar, A.; Tan, K.; Liu, J.; Kim, M.; Sun, Z. J.; Wagner, G.; Reinherz, E. L. Structure of a heterophilic adhesion complex between the human CD2 and CD58 (LFA-3) counterreceptors. *Cell* **1999**, *97*, 791–803.

(9) Bachmann, M. F.; Barner, M.; Kopf, M. CD2 sets quantitative thresholds in T cell activation. *J. Exp. Med.* **1999**, *190*, 1383–1391.

(10) Aruffo, A.; Hollenbaugh, D. Therapeutic intervention with inhibitors of co-stimulatory pathways in autoimmune disease. *Curr. Opin. Immunol.* **2001**, *13*, 683–686.

(11) da Silva, A. J.; Brickelmaier, M.; Majeau, G. R.; Li, Z.; Su, L.; Hsu, Y. M.; Hochman, P. S. Alefacept, an immunomodulatory recombinant LFA-3/IgG1 fusion protein, induces CD16 signaling and CD2/CD16-dependent apoptosis of CD2+ cells. *J. Immunol.* **2002**, *168*, 4462–4471.

(12) Hoffmann, J. C.; Herklotz, C.; Zeidler, H.; Bayer, B.; Rosenthal, H.; Westermann, J. Initiation and perpetuation of rat adjuvant arthritis is inhibited by the anti-CD2 monoclonal antibody (mAb) OX34. *Ann. Rheum. Dis.* **1997**, *56*, 716–722.

(13) Sido, B.; Dengler, T. J.; Otto, G. Differential immunosuppressive activity of monoclonal CD2 antibodies on allograft rejection versus specific antibody production. *Eur. J. Immunol.* **1998**, *28*, 1347–1357.

(14) Mrowietz, U. Treatment targeted to cell surface epitopes. *Clin. Exp. Dermatol.* **2002**, *27*, 591–596.

(15) Braun, J.; Sieper, J. Role of novel biological therapies in psoriatic arthritis: effects on joints and skin. *BioDrugs* **2003**, *17*, 187–199.

(16) Przepiorka, D.; Phillips, G. L.; Ratanatharathorn, V.; Cottler-Fox, M.; Sehn, L. H.; Antin, J. H.; LeBherz, D.; Awwad, M.; Hope, J.; McClain, J. B. A phase II study of BTI-322, a monoclonal anti-CD2 antibody, for treatment of steroid-resistant acute graft-versus-host disease. *Blood* **1998**, *92*, 4066–4071.

(17) Squifflet, J. P.; Besse, T.; Malaise, J.; Mourad, M.; Delcorde, C.; Hope, J. A.; Pirson, Y. BTI-322 for induction therapy after renal transplantation: a randomized study. *Transplant. Proc.* **1997**, *29*, 317–319.

(18) Besse, T.; Malaise, J.; Mourad, M.; Pirson, Y.; Hope, J.; Awwad, M.; White-Scharf, M.; Squifflet, J. P. Prevention of rejection with BTI-322 after renal transplantation (results at 9 months). *Transplant. Proc.* **1997**, *29*, 2425–2426.

(19) Spitzer, T. R.; McAfee, S. L.; Dey, B. R.; Colby, C.; Hope, J.; Grossberg, H. T. R.; Preffer, F.; Shaffer, J.; Alexander, S. I.; Sachs, D. H.; Sykes, M. Nonmyeloablative haploidentical stem-cell transplantation using anti-CD2 monoclonal antibody (MEDI-507)-based conditioning for refractory hematologic malignancies. *Transplantation* **2003**, *75*, 1748–1751.

(20) Ulbrich, H.; Eriksson, E. E.; Lindbom, L. Leukocyte and endothelial cell adhesion molecules as targets for therapeutic interventions in inflammatory disease. *Trends Pharmacol. Sci.* **2003**, *24*, 640–647.

(21) Anderson, M. E.; Siahaan, T. J. Targeting ICAM-1/LFA-1 interaction for controlling autoimmune diseases: designing peptide and small molecule inhibitors. *Peptides* **2003**, *24*, 487–501.

(22) Jois, S. D.; Jining, L.; Nagarajarao, L. M. Targeting T-cell adhesion molecules for drug-design. *Curr. Pharm. Des.* **2006**, *12*, 2797–2812.

(23) Jining, L.; Makagiansar, I.; Yusuf-Makagiansar, H.; Chow, V. T.; Siahaan, T. J.; Jois, S. D. Design, structure and biological activity of beta-turn peptides of CD2 protein for inhibition of T-cell adhesion. *Eur. J. Biochem.* **2004**, *271*, 2873–2886.

(24) Liu, J.; Ying, J.; Chow, V. T.; Hruby, V. J.; Satyanarayanajois, S. D. Structure−activity studies of peptides from the "hot spot" region of human CD2 protein: development of peptides for immunomodulation. *J. Med. Chem.* **2005**, *48*, 6236–6249.

(25) Liu, J.; Li, C.; Ke, S.; Satyanarayanajois, S. D. Structure-based rational design of beta-hairpin peptides from discontinuous epitopes of cluster of differentiation 2 (CD2) protein to modulate cell adhesion interaction. *J. Med. Chem.* **2007**, *50*, 4038–4047.

(26) Li, C.; Satyanarayanajois, S. D. Structure−function studies of peptides for cell adhesion inhibition: identification of key residues by alanine mutation and peptide-truncation approach. *Peptides* **2007**, *28*, 1498–1508.

(27) Blanco, F. J.; Jimenez, M. A.; Herranz, J.; Rico, M.; Santoro, J.; Nieto, J. L. NMR evidence of a short linear peptide that folds into a β-turn in aqueous solution. *J. Am. Chem. Soc.* **1993**, *115*, 5887–5888.

(28) Hutchinson, E. G.; Thronton, J. A revised set of potentials for β-turn formation in proteins. *Protein Sci.* **1994**, *3*, 2207–2216.

(29) Fesinmeyer, R. M.; Hudson, F. M.; Olsen, K. A.; White, G. W.; Euser, A.; Andersen, N. H. Chemical shifts provide fold populations and register of beta hairpins and beta sheets. *J. Biomol. NMR.* **2005**, *33*, 213–231.

(30) Liu, J.; Chow, V. T.; Jois, S. D. A novel, rapid and sensitive heterotypic cell adhesion assay for CD2−CD58 interaction, and its application for testing inhibitory peptides. *J. Immunol. Methods* **2004**, *291*, 39–49.

(31) Albert-Wolf, M.; Meuer, S. C.; Wallich, R. Dual function of recombinant human CD58: inhibition of T-cell adhesion and activation via the CD2 pathway. *Int. Immunol.* **1991**, *3*, 1335–1347.

(32) Mosmann, T. Rapid colorimetric assay for cellular growth and survival: application to proliferation and cytotoxicity assays. *J. Immunol. Methods* **1983**, *5*, 55–63.

(33) Perczel, A.; Fasman, G. D. Analysis of the circular dichroism spectrum of proteins using the convex constraint algorithm: a practical guide. *Anal. Biochem.* **1992**, *203*, 83–93.

(34) Perczel, A.; Fasman, G. D. Quantitative analysis of cyclic β-turn models. *Protein Sci.* **1992**, *1*, 378–395.

(35) Mahalakshmi, R.; Ragothama, S.; Balaram, P. NMR analysis of aromatic interactions in designed peptide β-hairpins. *J. Am. Chem. Soc.* **2006**, *128*, 1125–1138.

(36) Dyer, R. B.; Maness, S. J.; Franzen, S.; Fesinmeyer, R. M.; Olsen, K. A.; Andersen, N. H. Hairpin folding dynamics: the cold-denatured state is predisposed for rapid refolding. *Biochemistry* **2005**, *44*, 10406–10415.

(37) Bax, A.; Davis, D. G. MLEV-17-based two-dimensional homonuclear magnetization transfer spectroscopy. *J. Magn. Reson.* **1985**, *65*, 355–360.

(38) Bax, A.; Davis, D. G. Practical aspects of two-dimensional transverse NOE spectroscopy. *J. Magn. Reson.* **1985**, *63*, 207–213.

(39) Francart, C.; Wieruszeski, J. M.; Tartar, A.; Lippens, G. Structural and dynamic characterization of Pro *cis/trans* isomerization in a small cyclic peptide. *J. Am. Chem. Soc.* **1996**, *118*, 7019–7027.

(40) Bundi, A.; Wuthrich, K. ^{1}H NMR parameters of common amino acid residues measured in aqueous solution of linear tetrapeptide H-Gly-Gly-X-Ala-OH. *Biopolymers* **1979**, *18*, 285–297.

(41) Wishart, D. S.; Sykes, B. D.; Richards, F. M. The chemical shift index: a fast and simple method for the assignment of protein secondary structure through NMR spectroscopy. *Biochemistry.* **1992**, *31*, 1647–1651.

(42) Wuthrich, K. *NMR of Proteins and Nucleic Acids*; John Wiley & Sons: New York, 1986.

(43) Andersen, N. H.; Neidigh, J. W.; Harris, S. M.; Lee, G. M.; Liu, Z.; Tong, H. Extracting information from the temperature gradients of polypeptide NH chemical shifts. 1. The importance of conformational averaging. *J. Am. Chem. Soc.* **1997**, *119*, 8547–8561.

(44) Rose, G. D.; Gierasch, L. M.; Smith, J. A. Turns in peptides and proteins. *Adv. Protein Chem.* **1985**, *37*, 1–109.

(45) Constantine, K. L.; Mueller, L.; Andersen, N. H.; Tong, H.; Wandler, C. F.; Friedrichs, M. S.; Bruccoleri, R. E. Structural and dynamics properties of a β-hairpin-forming linear peptide. 1. Modeling using ensemble averaged constraints. *J. Am. Chem. Soc.* **1995**, *117*, 10841–10854.

(46) Anderson, N. H.; Olsen, K. A.; Fesinmeyer, M.; Tan, X.; Hudson, M. F.; Eidenschink, L. A.; Farazi, S. R. Minimization and optimization of designed β-hairpin folds. *J. Am. Chem. Soc.* **2006**, *128*, 6101–6110.

(47) Kim, M.; Sun, Z. Y.; Byron, O.; Campbell, G.; Wagner, G.; Wang, J.; Reinherz, E. L. Molecular dissection of the CD2−C58 counter-receptor interface identifies CD2 Tyr86 and CD58 Lys34 residues as the functional "hot spot". *J. Mol. Biol.* **2001**, *312*, 711–720.

(48) Gunasekaran, K.; Gomathi, L.; Ramakrishnan, C.; Chandrasekhar, J.; Balaram, P. Conformational interconversions in peptide β-turns: analysis of turns in proteins and computational estimates of barriers. *J. Mol. Biol.* **1998**, *284*, 1505–1516.

(49) Rietman, B. H.; Folkers, P. J. M.; Folmer, R. H. A.; Tesser, G. I.; Hilbers, C. W. The solution structure of the synthetic circular peptide CGVSRQGKPYC. NMR studies of the folding of a synthetic model for the DNA-binding loop of the ssDNA-binding protein encoded by gene V of phage M13. *Eur. J. Biochem.* **1996**, *238*, 706–713.

(50) McDonnell, J. M.; Fushman, D.; Cahill, S. M.; Sutton, B. J.; Cowburn, D. Solution structure of $Fc_{\epsilon}R1$ α-chain mimics: a β-hairpin peptide and its retroenantiomer. *J. Am. Chem. Soc.* **1997**, *119*, 5321–5328.

(51) de Alba, E.; Rico, M.; Jimenez, M. A. The turn sequence directs beta-strand alignment in designed beta-hairpins. *Protein Sci.* **1999**, *8*, 2234–2244.

(52) Hruby, V. J. Designing peptide receptor agonists and antagonists. *Nat. Rev. Drug Discovery* **2002**, *1*, 847–858.

(53) Santiveri, C. M.; Leon, E.; Rico, M.; Jimenez, M. A. Context-dependence of the contribution of disulfide bonds to beta-hairpin stability. *Chemistry* **2008**, *14*, 488–499.

(54) Schumann, C.; Seyfarth, L.; Greiner, G.; Paegelow, I.; Reissmann, S. Synthesis and biological activity of new side chain and backbone cyclic bradykinin analogues. *J. Pept. Res.* **2003**, *60*, 128–140.

(55) *Handbook of Combinatorial and Solid Phase Organic Chemistry: A Guide to Principles, Products and Protocols*; Advanced Chemtech: Louisville, KY, 1998; pp 329−372.

(56) Lloyd-Williams, P.; Albericio, F.; Giralt, E. *Chemical Approaches to the Synthesis of Peptides and Proteins*; CRC: Boca Raton, FL, 1997; pp 19−82.

(57) Gines, S.; Marino, M.; Mallol, J.; Canela, E. I.; Morimoto, C.; Callebaut, C.; Hovanessian, A.; Casado, V.; Lluis, C.; Franco, R.

Regulation of epithelial and lymphocyte cell adhesion by adenosine deaminase−CD26 interaction. *Biochem. J.* **2002**, *361*, 203–209.
(58) *InsightII*; Accelrys, Inc.: San Diego, CA. InsightII is a commercial, licensed molecular modeling software obtained from Accelrys, Inc. http://www.accelrys.com/products/insight/.
(59) Sutcliffe, M. J. Structure Determination from NMR Data II. Computational Approaches. In *NMR of Macromolecules: A Practical Approach*; Roberts, G. C. K., Ed.; Oxford University Press: New York, 1993; pp 359−390.
(60) Davis, I. W.; Leaver-Fay, A.; Chen, V. B.; Block, J. N.; Kapral, G. J.; Wang, X.; Murray, L. W., 3rd.; Snoeyink, J.; Richardson, J. S.; Richardson, D. C. MolProbity: all-atom contacts and structure validation for proteins and nucleic acids. *Nucleic Acids Res.* **2007**, *35*, W375–W383.
(61) Koradi, R.; Billeter, M.; Wüthrich, K. MOLMOL: a program for display and analysis of macromolecular structures. *J. Mol. Graphics* **1996**, *14*, 51–55.
(62) Srinivasan, N.; Sowdhamini, R.; Ramakrishnan, C.; Balaram, P. Conformations of disulfide bridges in proteins. *Int. J. Pept. Protein Res.* **1990**, *36*, 147–155.
(63) Rance, M.; Sorensen, O. W.; Bodenhausen, G.; Wagner, G.; Ernst, R. R.; Wüthrich, K. Improved spectral resolution in COSY ^{1}H NMR spectra of protein via double quantum filtering. *Biochem. Biophys. Res. Commun.* **1983**, *117*, 479–485.
(64) Goddard, T. D.; Kneller, D. G. *SPARKY3*; University of California: San Francisco, CA; http://www.cgl.ucsf.edu/home/sparky/.

JM8008212